

**Spectroscopy and lifetime measurements in  $^{66}\text{Ge}$ ,  $^{69}\text{Se}$ , and  $^{65}\text{Ga}$  using fragmentation reactions**

A. J. Nichols, R. Wadsworth,<sup>\*</sup> M. A. Bentley, P. J. Davies, J. Henderson, D. G. Jenkins, and I. Paterson  
*Department of Physics, University of York, Heslington, York YO10 5DD, United Kingdom*

H. Iwasaki, A. Lemasson,<sup>†</sup> V. M. Bader, T. Baugher, D. Bazin, J. S. Berryman, A. Gade, C. Morse, S. R. Stroberg,  
 D. Weisshaar, K. Whitmore, and K. Wimmer<sup>‡</sup>  
*National Superconducting Cyclotron Laboratory and Department of Physics and Astronomy,  
 Michigan State University, 640 S. Shaw Lane, East Lansing, Michigan 48824-1321, USA*

G. de Angelis  
*Laboratori Nazionali di Legnaro dell'INFN, Legnaro (Padova) I-35020, Italy*

A. Dewald, T. Braunroth, C. Fransen, and M. Hackstein  
*Institut für Kernphysik der Universität zu Köln, Köln D-50937, Germany*

D. Miller<sup>§</sup>  
*Department of Physics and Astronomy, University of Tennessee, Knoxville, Tennessee 37996, USA*  
 (Received 12 September 2014; revised manuscript received 18 December 2014; published 21 January 2015)

Lifetimes of low-lying excited states have been measured in  $^{66}\text{Ge}$ ,  $^{69}\text{Se}$ , and  $^{65}\text{Ga}$  using a  $\gamma$ -ray lineshape method. The results confirm the previously reported  $7_1^-$  state lifetime in  $^{66}\text{Ge}$ . The lifetime of the yrast  $5/2^-$  state in  $^{65}\text{Ga}$  is measured for the first time. Lifetime measurements of two excited  $3/2^-$  states in  $^{69}\text{Se}$  are also reported. Two previously unobserved  $\gamma$  rays have been identified in  $^{69}\text{Se}$ .  $\gamma$ - $\gamma$  coincidence measurements have been used to place one of these in the level scheme.  $^{69}\text{Se}$  excited state populations are compared to shell-model calculations using the GXPF1A interaction in the  $fp$  model space. Theoretical spectroscopic factors to excited states in  $^{69}\text{Se}$  have identified three candidate levels for the origin of one of the new transitions.

DOI: [10.1103/PhysRevC.91.014319](https://doi.org/10.1103/PhysRevC.91.014319)

PACS number(s): 21.10.Tg, 23.20.-g, 25.70.-z, 27.50.+e

**I. INTRODUCTION**

Studies of  $A \sim 70$ ,  $N \sim Z$  nuclei have increased with the advent of fast radioactive ion beams. In these nuclei the valence nucleons may occupy orbitals in the  $fp$  shell, and the deformation-driving effects of the  $g_{9/2}$  intruder orbital [1,2] increase collectivity in this midshell region. This region is also of interest because of the complex interplay between stable prolate, oblate, and triaxial shapes. Here, nuclear shapes change rapidly with both nucleon number and angular momentum [3]. These effects arise from the presence of large subshell gaps at nucleon numbers of 34 and 36 (oblate), 34 and 38 (prolate), and 40 (spherical) [2,4].

It is well established that reduced transition matrix elements provide information on the collectivity of a nucleus. This is particularly important for  $A \sim 70$ ,  $N \sim Z$  nuclei as it can be used to highlight the contribution of the  $g_{9/2}$  intruder orbital. It is possible to determine such matrix elements from Coulomb excitation [5] or lifetime measurements of excited states. This

information is very useful as it can provide a stringent test of nuclear models. Examples of previous such studies in this region can be found in Refs. [6–13]. This paper discusses lifetime measurements of states in nuclei residing in the  $A \sim 70$ ,  $N \sim Z$  region:  $^{66}\text{Ge}$ ,  $^{69}\text{Se}$ , and  $^{65}\text{Ga}$ .

Previous studies of the nucleus  $^{66}\text{Ge}$  have observed excited states (e.g., [10,14]) and extracted properties, such as excited-state lifetimes and quadrupole moments [8,9]. These studies employed fusion-evaporation and Coulex reactions. In the case of  $^{65}\text{Ga}$  [7,15] fusion-evaporation reactions were used to populate excited states. The lifetimes of two low-lying states in  $^{69}\text{Se}$  were reported in Refs. [16,17].

This work presents lifetime measurements of two low-lying excited  $3/2^-$  states in  $^{69}\text{Se}$  and a lifetime measurement of the yrast  $5/2^-$  state in  $^{65}\text{Ga}$ . Excited states in  $^{69}\text{Se}$  are probed after population via single-neutron knockout for the first time in this work. The results for  $^{69}\text{Se}$  are compared to shell-model calculations. The technique used to extract lifetime values is tested with a re-measurement of the known  $7_1^-$  state lifetime in  $^{66}\text{Ge}$  [10,14].

**II. EXPERIMENTAL DETAILS**

The Coupled Cyclotron Facility [18] at the National Superconducting Cyclotron Laboratory (NSCL) produced a  $^{78}\text{Kr}$  primary beam at 150 MeV/u. This beam was fragmented on a 399 mg/cm<sup>2</sup>  $^9\text{Be}$  production target. The secondary  $^{70}\text{Se}$  and  $^{69}\text{As}$  beams produced from the fragmentation reaction

<sup>\*</sup>rw10@npg.york.ac.uk

<sup>†</sup>Present address: GANIL, CEA/DSM-CNRS/IN2P3, BP 55027, F-14076 Caen Cedex 5, France.

<sup>‡</sup>Present address: Department of Physics, University of Tokyo, Hongo, Bunkyo-ku, Tokyo 113-0033, Japan.

<sup>§</sup>Present address: TRIUMF, 4004 Wesbrook Mall, Vancouver, BC V6T 2A3, Canada.

were selected using the A1900 fragment separator [19], and had typical intensities (purities) of  $3.6 \times 10^5$  pps (38%) and  $3.8 \times 10^5$  pps (39%), respectively, after traversing the A1900. Isotonic secondary beams transmitted through the A1900 were separated cleanly via time-of-flight difference measured between two plastic scintillators placed before the secondary target position.

The  ${}^9\text{Be}({}^{70}\text{Se}, {}^{66}\text{Ge}\gamma)$ ,  ${}^9\text{Be}({}^{70}\text{Se}, {}^{69}\text{Se}\gamma)$ ,  ${}^9\text{Be}({}^{70}\text{Se}, {}^{65}\text{Ga}\gamma)$ , and  ${}^9\text{Be}({}^{69}\text{As}, {}^{65}\text{Ga}\gamma)$  reactions were used in this work. These reactions occurred at a secondary target of  $96 \text{ mg/cm}^2$   ${}^9\text{Be}$  housed at the target position of the S800 spectrograph [20]. The reaction products left the target foil with velocities of approximately  $0.39c$  and were subsequently transported into the focal plane of the S800 spectrograph [20]. In the S800, the Z and A/Q of the recoils were identified on an event-by-event basis from energy-loss and time-of-flight information using an ionization chamber and plastic scintillators, respectively. This identification provided recoil separation and allowed for clean software cuts on individual reaction products, resulting in negligible recoil contamination in the  $\gamma$ -ray spectra.

The SeGA germanium array [21] was utilized to detect de-excitation  $\gamma$  rays from the recoiling reaction products. SeGA is an array of segmented high-purity germanium detectors that surrounds the target position. In the present experiment, 7(8) SeGA detectors were placed at  $30^\circ$  ( $140^\circ$ ) to the beam direction to provide the maximum Doppler shift between  $\gamma$  rays detected in the two rings.

### III. RESULTS

#### A. $\gamma$ Spectroscopy

Full spectra showing the  $\gamma$  decays observed in coincidence with  ${}^{69}\text{Se}$  and  ${}^{65}\text{Ga}$  recoils are shown in Fig. 1. Partial level schemes for  ${}^{69}\text{Se}$  and  ${}^{65}\text{Ga}$  showing  $\gamma$  rays observed in this

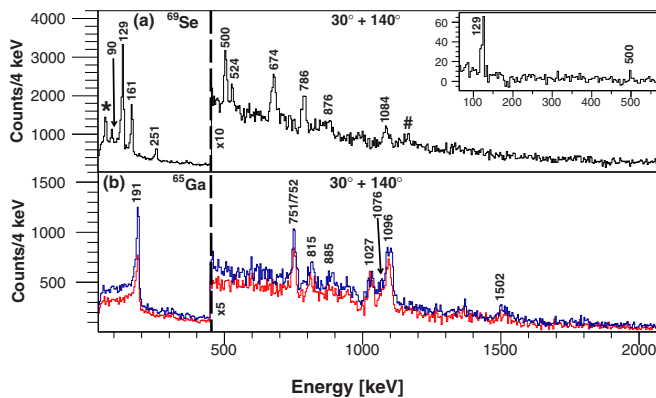


FIG. 1. (Color online) (a)  $\gamma$  spectrum from gating data on  ${}^{69}\text{Se}$  recoils for both SeGA angles. The peak labeled with a \* is a radiative electron capture x ray. The peak marked with a # is a contaminant peak from excitations in  ${}^{27}\text{Al}$  present in the target housing. (Inset) Target-only  $\gamma$  spectrum gated on the 161-keV transition. The 500-keV  $\gamma$  ray is observed to come in coincidence with the 129-keV and 161-keV transitions in  ${}^{69}\text{Se}$ . (b)  $\gamma$  spectrum from gating data on  ${}^{65}\text{Ga}$  recoils created via  $3p2n$  removal from the  ${}^{70}\text{Se}$  secondary beam (red) and via  $2p2n$  removal from the  ${}^{69}\text{As}$  secondary beam (blue). The observed transitions in both nuclei are labeled.

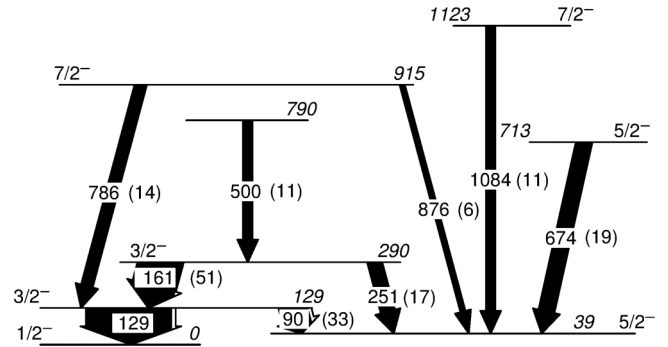


FIG. 2. Partial level scheme for  ${}^{69}\text{Se}$  identifying the levels populated in this work. The arrow thicknesses correspond to the relative intensities of the transitions (the 129-keV transition is set to 100), which are quantified by the values in brackets. The newly assigned state is shown at 790 keV.

work are presented in Figs. 2 and 3, respectively, and are assigned based on the known level schemes. The higher spin of states observed in  ${}^{65}\text{Ga}$  relative to  ${}^{69}\text{Se}$  is consistent with its population resulting from multinucleon removal, compared to one-neutron knockout in the case of  ${}^{69}\text{Se}$ .

No new transitions were observed in  ${}^{66}\text{Ge}$  or  ${}^{65}\text{Ga}$  from the reactions used in this work. Furthermore, no evidence was found for the population of the known low-lying positive-parity states in  ${}^{69}\text{Se}$ . This is in line with expectation, as previous work supports a lack of significant  $g_{9/2}$  orbital nucleon occupation in the ground state of  ${}^{70}\text{Se}$  [12]. The  $3/2^-$  state at 290 keV in  ${}^{69}\text{Se}$  is fed by a 500(3)-keV transition from a state of an unknown spin parity, which was located with  $\gamma$ - $\gamma$  coincidence measurements for the first time in this work. A coincidence spectrum gated on the 161-keV transition in  ${}^{69}\text{Se}$

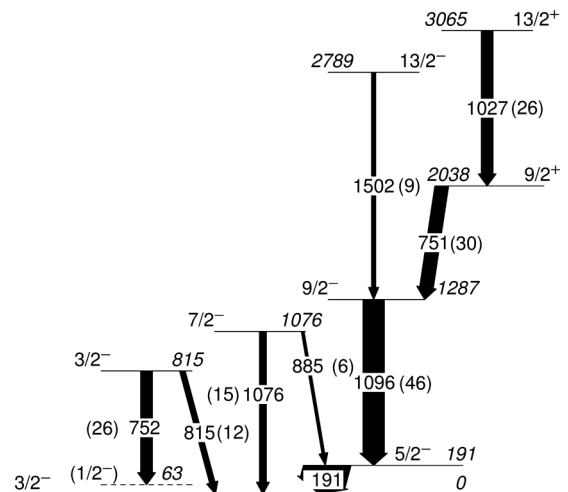


FIG. 3. Partial level scheme for  ${}^{65}\text{Ga}$  identifying the levels populated in this work. The arrow thicknesses correspond to the relative intensities of the transitions (the 191-keV transition is set to 100), which are quantified by the values in brackets (taken from weighted average contributions of  ${}^{65}\text{Ga}$  excited via two reaction mechanisms; see text). Levels with tentatively assigned spin parities in the literature are shown in parenthesis and with a dashed level.

TABLE I. Initial and final level spin parities ( $J_{i,f}^\pi$ ), level energies ( $E_{i,f}$ ),  $\gamma$ -ray energies ( $E_\gamma$ ), measured mean state lifetimes ( $\tau_m$ ), and corresponding reduced transition strengths ( $B(\lambda L \downarrow)$ ) studied in this work. The table contains both present results (Pres.) and previously published results (Lit.). A theoretical  $B(M1 \downarrow)$  value is included from shell-model calculations (Theo.). The errors quoted include both statistical and systematic effects.

	$J_i^\pi$	$E_i$ (keV)	$J_f^\pi$	$E_f$ (keV)	$E_\gamma$ (keV)	Mult.	$\tau_m$ (ps)		$B(M1 \downarrow)(\mu_N^2)$			$B(E2 \downarrow) (e^2\text{fm}^4)$	
							Pres.	Lit.	Pres.	Lit.	Theo.	Pres.	Lit.
$^{66}\text{Ge}$	$7_1^-$	4205	$5_1^-$	3683	521	$E2$	281(44)	276(13) <sup>a</sup>	76(12)	77(4) <sup>a</sup>	–	–	–
$^{69}\text{Se}$	$3/2_2^-$	290	$3/2_1^-$	129	161	$M1$	325(16)	–	0.031(3)	–	0.005	–	–
	$3/2_2^-$	290	$5/2_1^-$	34	251	$M1/E2$	360(28)	–	–	–	–	–	–
	$3/2_1^-$	129	$1/2_{gs}^-$	0.0	129	$M1/E2$	380(18)	–	–	–	–	–	–
$^{65}\text{Ga}$	$5/2_1^-$	191	$3/2_{gs}^-$	0.0	191	$M1/E2$	938(34)	$\leq 1010^b$	0.0058(23)	$\geq 0.0053^b$	–	1120(220)	$\geq 1039^b$

<sup>a</sup>From [9].

<sup>b</sup>Using [7,15].

is shown in the inset of Fig. 1(a). The previously unobserved 524(3)-keV transition identified in this work was too weak for coincidence measurements to locate its position in the known level scheme. See Fig. 2 for details of  $\gamma$ -ray intensities observed in  $^{69}\text{Se}$ .

$^{65}\text{Ga}$  was produced via multiple-nucleon removal from both the  $^{70}\text{Se}$  and  $^{69}\text{As}$  secondary beams. The  $\gamma$ -ray intensities from states in  $^{65}\text{Ga}$  populated via the two reaction mechanisms were measured separately and found to be similar within experimental error (see Fig. 1). For example, from the  $\gamma$  spectrum associated with  $^{65}\text{Ga}$  populated from the  $^{70}\text{Se}$  secondary beam, the 1096-keV  $9/2^- \rightarrow 5/2^-$   $\gamma$  ray was measured to be 42(11)% of the intensity of the subsequent decay to the ground state via the 191-keV  $5/2^- \rightarrow 3/2^-$  transition. The same 1096-keV transition was measured in the  $^{65}\text{Ga}$   $\gamma$  spectrum populated from the  $^{69}\text{As}$  secondary beam to be 59(21)% of the intensity of the 191-keV transition. The  $\gamma$ -ray intensities for  $^{65}\text{Ga}$  in this work are taken as the weighted average measured intensities of the spectra from the two reaction mechanisms because they both involve similar multinucleon removal reactions. These intensities are presented in Fig. 3.

## B. Lifetime results

Excited-state lifetimes in this work were extracted using the  $\gamma$ -ray lineshape method [22–24], which is based on the emission-point distribution of  $\gamma$  rays from recoiling nuclei. Lifetimes were extracted by comparing the experimental  $\gamma$ -ray lineshape spectra to simulations generated using a dedicated lifetime code developed at NSCL [22], which utilizes the GEANT4 framework [25]. Reference [26] discusses the use and validity of simulations of this type. The simulations can be tailored to accurately replicate the experimental setup by fitting simulated particle spectra, such as recoil velocity distributions, to their experimental equivalents. The simulation package allows for accurate consideration of lifetimes of feeding states and  $\gamma$ -ray intensities. Simulated  $\gamma$ -ray spectra with varying lifetimes are then compared with experimental data. A background was added to the simulations to accurately replicate the experimental background in the region of lifetime sensitivity. In this work, exponential backgrounds were fitted to the spectra for forward-ring data. For data taken at backward SeGA angles,

a combination of second-order polynomial and exponential background was used, the second-order polynomial being used to replicate the low-energy background. Data taken at forward and backward SeGA angles were analyzed separately, with the final lifetime result comprising the weighted average of results from the two rings. Fits to data taken at backward SeGA angles were found to be less sensitive to state lifetimes than forward-ring data, however, results from forward and backward SeGA rings agreed within experimental error. For state lifetimes measured in this work, efforts were made to extract the effective lifetimes of dominant feeding states so they could be taken into account in the analysis. These are discussed further below.

The results extracted in this work are displayed in Table I. The errors quoted for all results in this work include both statistical uncertainties and systematic errors. Systematic errors were determined using simulations. This was achieved by setting each dependent parameter to one standard deviation away from its measured value and re-analyzing the lifetime of the state of interest. The most significant contributions to the systematic errors in this work came from uncertainties in the lifetimes of feeding states, feeding transition intensities, and assumptions regarding the location of the background. Uncertainties in the coefficients of the functions used to determine the background location were given errors of 5% because larger variations resulted in noticeably incorrect background fits.

The validity of the  $\gamma$ -ray lineshape method was tested via a measurement of the  $^{66}\text{Ge}$   $7_1^-$  state lifetime. The  $7_1^-$  state was observed to be fed by the 338-keV transition from the known  $7_2^-$  state [14], with an intensity of 24(5)% relative to the depopulating  $7_1^- \rightarrow 5_1^-$  transition. No transitions were observed to populate the  $7_2^-$  state. The lifetime of the  $7_2^-$  state in the literature is quoted as 86(6) ps [14]. Because of insufficient statistics, it was not possible to measure the lifetime of the  $7_2^-$  state in this work, therefore the simulations were generated assuming the literature  $7_2^-$  state lifetime. The  $7_1^-$  state lifetime in  $^{66}\text{Ge}$  extracted in this work is  $\tau(7_1^-) = 281 \pm 42(\text{stat}) \pm 17(\text{sys})$  ps, giving a corresponding reduced transition strength  $B(E2; 7_1^- \rightarrow 5_1^-) = 76(12) e^2\text{fm}^4$  (statistical and systematic uncertainties have been combined). These values are in excellent agreement with the weighted average of the literature values [10,14].

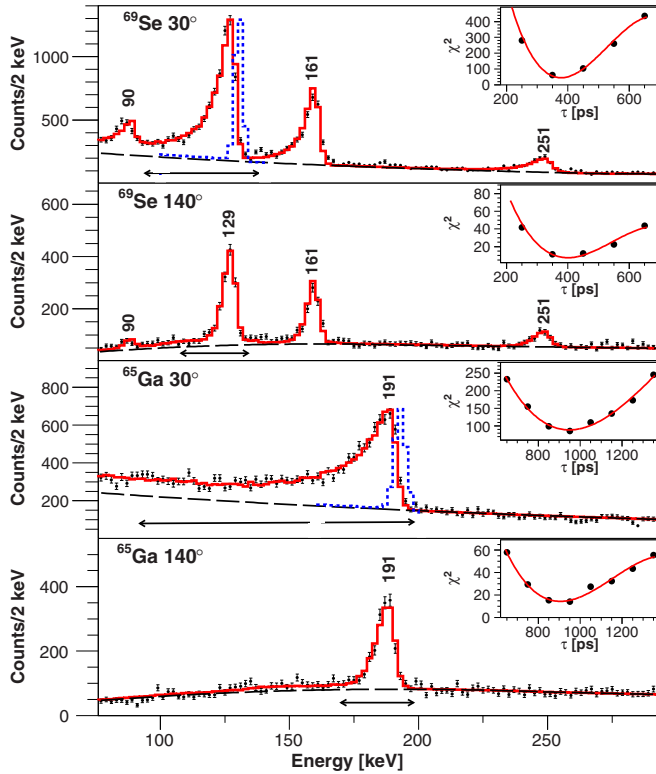


FIG. 4. (Color online) Doppler-shift corrected  $\gamma$ -ray spectra obtained for  $^{69}\text{Se}$  (top two panels) and  $^{65}\text{Ga}$  (bottom two panels). The simulated fits to the  $\gamma$  spectra are shown (red line), along with background fits (dashed black line). Arrows denote the region of lifetime sensitivity used in the extraction of the  $3/2^-$  state at 129 keV in  $^{69}\text{Se}$  and the  $5/2^-$  state at 191 keV in  $^{65}\text{Ga}$ . The dotted blue lines show simulations of forward-angle data for the 129-keV state in  $^{69}\text{Se}$  and the 191-keV state in  $^{65}\text{Ga}$  assuming a lifetime of 0 ps. The insets to the spectra show the  $\chi^2$ -minimization plots used to determine the lifetimes of the 129-keV state in  $^{69}\text{Se}$  and the 191-keV state in  $^{65}\text{Ga}$ .

Because of insufficient statistics, it was not possible to ascertain the lifetime of the newly observed state at  $E_x = 790$  keV in  $^{69}\text{Se}$ . The lifetime of the  $3/2^-$  state at 290 keV was obtained assuming a negligible delay from feeding resulting from this new state because it has a relatively weak feeding contribution and no lifetime is known. The 290-keV state is observed to decay via two  $\gamma$  transitions in this work (see Fig. 2).  $\gamma$ -ray lineshape fits were made to the 161-keV and the 251-keV transitions (see Fig. 4). The resulting weighted mean lifetime from fits to both depopulating transitions is  $\tau(290 \text{ keV}) = 332 \pm 12(\text{stat}) \pm 9(\text{sys})$  ps. The multipole mixing ratio of the 161-keV transition, extracted via a directional correlation from oriented states (DCO) measurement [16], determined the transition to be pure dipole in character. Therefore, the  $B(M1 \downarrow)$  for this transition, taking into account the branching ratio from the 290-keV state measured in the present work, was determined to be  $0.031(3) \mu_N^2$ .

The  $3/2^-$  state at 129 keV in  $^{69}\text{Se}$  was observed to decay to the ground state via the 129-keV transition and to the  $5/2^-$  state at 39 keV via the 90-keV transition (see Fig. 2). The lifetime of the  $3/2^-$  state at 129 keV was analyzed assuming the lifetime

of the  $7/2^-$  feeding state at 915 keV was negligible, as it is not known and its feeding contribution is much less than the contribution from the 290-keV state. However, the measured lifetime of the  $3/2^-$  state at 290 keV and the measured feeding intensity of the 161-keV  $\gamma$  ray [51(3)%] were taken into account as they have been measured in this work. The lifetime of the  $3/2^-$  state at 129 keV was extracted from simulated fits to the 129-keV transition. The lifetime deduced from these fits is  $380 \pm 9(\text{stat}) \pm 16(\text{sys})$  ps; see Fig. 4. The lifetime of the  $3/2^-$  state at 129 keV could not be extracted via a fit to the 90-keV transition because of a lack of sensitivity to lifetime in this low-energy region.

The lifetime of the  $5/2^-$  state at 191 keV in  $^{65}\text{Ga}$  was extracted assuming a negligible contribution from the feeding of higher-lying excited states. The lifetimes of the  $7/2^-$  state at 1076 keV and the  $9/2^-$  state at 1287 keV could not be extracted in the present work. Furthermore, the lifetime of the  $7/2^-$  state at 1076 keV is not known in the literature, however, it has a small feeding intensity of 6(2)% and so it was assumed in this work to have a negligible delaying effect (see Fig. 3). The  $9/2^-$  state at 1287 keV has a literature lifetime upper limit of  $\leq 2$  ps [7], which suggests that its contribution to the decay of the  $5/2^-$  state at 191 keV (with a lifetime of hundreds of picoseconds; see below) is also likely to be negligible, despite its relatively large feeding intensity of 46(10)%. Simulated fits are made to  $\gamma$ -ray spectra of  $^{65}\text{Ga}$  created from both  $^{70}\text{Se}$  and  $^{69}\text{As}$  secondary beams added together (see Fig. 4). The result of  $\tau(191 \text{ keV}) = 938 \pm 24(\text{stat}) \pm 24(\text{sys})$  ps is consistent with the upper limit given in the literature of  $\tau(191 \text{ keV}) \leq 1010$  ps [7]. Assuming an  $E2/M1$  mixing ratio  $\delta$  of  $-0.7(3)$ , a feature supported by angular distribution of oriented states measurements for the 191-keV transition [15], gives a corresponding  $B(M1 \downarrow) = 0.0058(23) \mu_N^2$  and  $B(E2 \downarrow) = 1120(220) \text{ e}^2\text{fm}^4$ . The  $B(M1 \downarrow)$  and  $B(E2 \downarrow)$  values extracted in this work are consistent with the literature limits of  $\geq 0.0053 \mu_N^2$  and  $\geq 1039 \text{ e}^2\text{fm}^4$ , respectively [7,15].

#### IV. DISCUSSION

Because analysis of the  $^{69}\text{Se}$   $\gamma$  spectrum indicated the presence of previously unobserved transitions (see Fig. 1), level energies and occupations in  $^{69}\text{Se}$  were investigated with shell-model calculations using the ANTOINE code [27]; see Table II. Calculations were performed using the GXPF1A interaction [28,29] in the  $fp$  model space, truncated to allow up to five particle-hole excitations from the  $f_{7/2}$  orbital [30]. Table II contains predicted spectroscopic factors (S.F.) and excitation energies  $E_{\text{theo}}$ . Based on theoretical spectroscopic factors and a comparison between experimental and predicted level energies, certain states have been attributed to those experimentally observed ( $E_{\text{exp}}$ ). The shell-model calculations correctly predict the experimentally deduced  $1/2^-$  ground state of  $^{69}\text{Se}$  [31] (see Table II). The calculations also predict a significant population of the  $5/2^-$  state in  $^{69}\text{Se}$ , however, the decay from this state is not seen experimentally because of its long mean lifetime [2.9(3)  $\mu\text{s}$  [32]] and low  $\gamma$ -ray energy (39 keV, which is below the SeGA energy threshold). The calculations predict a vanishingly small population of the  $7/2^-$  state, with larger populations of the  $7/2^-$  and

TABLE II. Shell-model calculations for one-neutron knockout to negative-parity excited states in  $^{69}\text{Se}$  using the GXPF1A interaction in a truncated  $fp$  model space. Quoted are predicted spectroscopic factors (S.F.) and excitation energies ( $E_{\text{theo}}$ ). Experimentally observed excited states have been assigned ( $E_{\text{exp}}$ ). Tentative assignments in the  $E_{\text{exp}}$  column are quoted in parentheses.

$J$	$N$	S.F.	$E_{\text{theo}}$ (keV)	$E_{\text{exp}}$ (keV)
1/2	1	0.307	0.0	0.0
3/2	1	0.060	110	129
5/2	1	2.102	133	39
3/2	2	0.956	534	290
3/2	3	0.005	692	(790)
5/2	2	0.186	753	713
7/2	1	0.000	885	–
1/2	2	0.340	978	(790)
5/2	3	0.005	1109	(790)
7/2	2	0.095	1163	915
5/2	4	0.025	1322	–
7/2	3	0.267	1391	1123
3/2	4	0.016	1548	–

$7/2_3^-$  states. In Table II it was assumed, therefore, that the spectroscopic factors to the  $7/2_2^-$  and  $7/2_3^-$  states in the calculations correspond to the experimentally observed 915-keV and 1123-keV  $7/2^-$  states, respectively.

As indicated in Table II, three candidate states ( $1/2_2^-$ ,  $3/2_3^-$ , and  $5/2_3^-$ ) have been selected as potentially giving rise to the previously unobserved 500(3)-keV  $\gamma$  transition in  $^{69}\text{Se}$ . The  $1/2_2^-$  state predicted in the shell-model calculations has a much larger associated spectroscopic factor than the other two candidate states (see Table II) in this truncated model space, suggesting that this assignment for the new state is most likely. However, neither of the other two possible states can be excluded. Any of the three spin parities proposed for this new state would help to explain why it was not observed previously, as past studies have employed a fusion-evaporation reaction (which tends to populate mainly near yrast states, e.g., [16,17]).

The 161-keV transition in  $^{69}\text{Se}$  was determined to be essentially pure dipole in character [16]. The  $B(M1 \downarrow)$  value

for this transition is small (see Table I), suggesting a hindered nature. Shell-model calculations performed using ANTOINE predict hindered dipole transitions for low-lying excited states in  $^{69}\text{Se}$ , in line with what is experimentally deduced. The  $B(M1 \downarrow)$  predicted for the 161-keV transition in  $^{69}\text{Se}$  is  $0.005 \mu_N^2$ , which is an order of magnitude smaller than the experimentally deduced value (see Table I). Other low-lying dipole transitions of odd-mass nuclei in this region have been identified as hindered; for example, the decay in  $^{67}\text{Ga}$  from the 829-keV  $3/2^-$  state to the 167-keV  $1/2^-$  state was shown to have an associated  $B(M1 \downarrow)$  of  $0.06(1) \mu_N^2$  [33]. This is in reasonable agreement with a theoretical value quoted in Ref. [33] of  $0.04 \mu_N^2$ , obtained from three-particle cluster core model calculations. Hindered transitions in  $^{67}\text{Ga}$  have also been explained using particle-phonon coupling model calculations [34,35].

## V. SUMMARY

The  $\gamma$ -ray lineshape method was used in combination with single-nucleon knockout and multiple-nucleon removal reactions to obtain lifetime measurements for the  $7_1^-$  state in  $^{66}\text{Ge}$ , the  $3/2_1^-$  and  $3/2_2^-$  states in  $^{69}\text{Se}$ , and the  $5/2_1^-$  state in  $^{65}\text{Ga}$ . The  $^{66}\text{Ge}$   $7_1^-$  lifetime result is consistent with previous measurements.  $\gamma$ - $\gamma$  coincidence measurements identified a new 500(3)-keV transition in  $^{69}\text{Se}$ , feeding the  $3/2_2^-$  state from a previously unknown excited state. Shell-model calculations for  $^{69}\text{Se}$  using the GXPF1A interaction in a truncated  $fp$  model space were found to give excited-state populations that were reasonably consistent with experimental work. The shell-model calculations identified three candidates for the new 790-keV state in  $^{69}\text{Se}$ , the most likely of which being the previously unobserved  $1/2_2^-$  state.

## ACKNOWLEDGMENTS

This work is supported by the National Science Foundation (NSF) under Grant No. PHY-1102511, the Department of Energy (DOE) National Nuclear Security Administration under Awards No. DE-NA0000979 and No. DE-FG02-96ER40983, BMBF(Germany) under Contract No. 05P12PKFNE, and the UK STFC, No. ST/J000124/1.

- 
- [1] M. Hasagawa *et al.*, *Phys. Lett. B* **656**, 51 (2007).
  - [2] W. Nazarewicz *et al.*, *Nucl. Phys. A* **435**, 397 (1985).
  - [3] Y. Fu, H. Mei, J. Xiang, Z. P. Li, J. M. Yao, and J. Meng, *Phys. Rev. C* **87**, 054305 (2013).
  - [4] M. Bender, P. Bonche, and P.-H. Heenen, *Phys. Rev. C* **74**, 024312 (2006).
  - [5] A. Winther and K. Alder, *Nucl. Phys. A* **319**, 518 (1979).
  - [6] K. Starosta *et al.*, *Phys. Rev. Lett.* **99**, 042503 (2007).
  - [7] P. Banerjee *et al.*, *Il Nuovo Cim.* **110A**, 1365 (1997).
  - [8] A. Corsi *et al.*, *Phys. Rev. C* **88**, 044311 (2013).
  - [9] R. Lüttke *et al.*, *Phys. Rev. C* **85**, 017301 (2012).
  - [10] R. Wadsworth *et al.*, *J. Phys. G* **5**, 1761 (1979).
  - [11] A. Obertelli *et al.*, *Phys. Rev. C* **80**, 031304(R) (2009).
  - [12] A. Nichols *et al.*, *Phys. Lett. B* **733**, 52 (2014).
  - [13] A. Gade *et al.*, *Phys. Rev. Lett.* **95**, 022502 (2005).
  - [14] L. Cleeman *et al.*, *Nucl. Phys. A* **334**, 157 (1980).
  - [15] H. Kawakami *et al.*, *Phys. Rev. C* **21**, 1311 (1980).
  - [16] I. Stefanescu *et al.*, *Phys. Rev. C* **69**, 034333 (2004).
  - [17] D. G. Jenkins *et al.*, *Phys. Rev. C* **64**, 064311 (2001).
  - [18] P. Miller *et al.*, in *Proceedings of the 2001 Particle Accelerator Conference, Chicago* (IEEE, Piscataway, 2001), p. 2557.
  - [19] D. J. Morrissey *et al.*, *Nucl. Instr. Meth. Phys. Res. B* **204**, 90 (2003).
  - [20] D. Bazin *et al.*, *Nucl. Instr. Meth. Phys. Res. B* **204**, 629 (2003).
  - [21] W. F. Mueller *et al.*, *Nucl. Instr. Meth. Phys. Res. A* **466**, 492 (2001).
  - [22] A. Lemasson *et al.*, *Phys. Rev. C* **85**, 041303(R) (2012).
  - [23] J. R. Terry *et al.*, *Phys. Rev. C* **77**, 014316 (2008).
  - [24] P. Doornenbal *et al.*, *Nucl. Instr. Meth. Phys. Res. A* **613**, 218 (2010).
  - [25] S. Agostinelli *et al.*, *Nucl. Instr. Meth. Phys. Res. A* **506**, 250 (2003).

- [26] P. Adrich *et al.*, *Nucl. Instr. Meth. Phys. Res. A* **598**, 454 (2009).
- [27] E. Caurier and F. Nowacki, *Acta. Phys. Pol. B* **30**, 705 (1999).
- [28] M. Honma, T. Otsuka, B. A. Brown, and T. Mizusaki, *Phys. Rev. C* **65**, 061301 (2002).
- [29] M. Honma, T. Otsuka, B. A. Brown, and T. Mizusaki, *Phys. Rev. C* **69**, 034335 (2004).
- [30] P. G. Hansen and J. A. Tostevin, *Annu. Rev. Nucl. Part. Sci.* **53**, 219 (2003).
- [31] J. A. Macdonald *et al.*, *Nucl. Phys. A* **288**, 1 (1977).
- [32] C. D. Nesaraja, *Nuclear Data Sheets* **115**, 1 (2014).
- [33] T. P. Paradellis, *Nucl. Phys. A* **279**, 293 (1977).
- [34] A. M. Al-Naser *et al.*, *J. Phys. G* **3**, 1383 (1977).
- [35] A. M. Al-Naser *et al.*, *J. Phys. G* **4**, 1611 (1978).